Imaging the Environment of Green Fluorescent Protein

Klaus Suhling,* Jan Siegel,† David Phillips,‡ Paul M. W. French,† Sandrine Lévêque-Fort,† Stephen E. D. Webb,† and Daniel M. Davis*

*Department of Biological Sciences, Sir Alexander Fleming Building, †Photonics Group, The Blackett Laboratory, ‡Department of Chemistry, Imperial College of Science, Technology and Medicine, London, United Kingdom

ABSTRACT An emerging theme in cell biology is that cell surface receptors need to be considered as part of supramolecular complexes of proteins and lipids facilitating specific receptor conformations and distinct distributions, e.g., at the immunological synapse. Thus, a new goal is to develop bioimaging that not only locates proteins in live cells but can also probe their environment. Such a technique is demonstrated here using fluorescence lifetime imaging of green fluorescent protein (GFP). We first show, by time-correlated single-photon counting, that the fluorescence decay of GFP depends on the local refractive index. This is in agreement with the Strickler Berg formula, relating the Einstein *A* and *B* coefficients for absorption and spontaneous emission in molecules. We then quantitatively image, by wide-field time-gated fluorescence lifetime imaging, the refractive index of the environment of GFP. This novel approach paves the way for imaging the biophysical environment of specific GFP-tagged proteins in live cells.

INTRODUCTION

The green fluorescent protein (GFP) of the jellyfish *Aequorea victoria* (Tsien, 1998; Zimmer, 2002) is widely used in cell imaging applications (Sullivan and Kay, 1999) to reveal the location of proteins. However, such imaging of fluorescence intensity does not generally provide information about the environment of the protein. Fluorescence lifetime imaging (FLIM) (Lakowicz et al., 1992; Wang et al., 1992; Gadella et al., 1993; Scully et al., 1997; Bastiaens and Squire, 1999; Dowling et al., 1999) is a technique that, in addition to position and intensity, also captures the fluorescence lifetime. The fluorescence lifetime τ is the time a fluorophore remains in its excited state after excitation, and it is typically a few nanoseconds. τ is related to the radiative rate constant k_r and the nonradiative rate constant k_{nr} by

$$\frac{1}{\tau} = k_r + k_{nr}. \tag{1}$$

The fluorescence lifetime depends on the environment surrounding the fluorophore and can therefore be used to report on this environment. Indeed, using the fluorescence probe DPH in cell membranes, measurements of fluorescence lifetimes provided early evidence of heterogeneity in cell membranes (Klausner et al., 1980).

Recently, FLIM of the fluorescence decay of GFP has been used to report on the phosphorylation of GFP-tagged ErB1 receptors by identifying a shortened GFP fluorescence lifetime due to fluorescence resonance energy transfer (FRET) between the donor ErB1-GFP and a Cy3-labeled antibody to phosphortyrosine as the acceptor (Verveer et al., 2000). FLIM of FRET between the spectrally similar donor GFP and acceptor yellow fluorescent protein has also been used to monitor caspase activity in individual cells during apoptosis (Harpur et al., 2001). However, instead of using FLIM to report FRET, we demonstrate here that the GFP fluorescence decay could be directly used to probe the local environment of GFP.

The refractive index of the medium surrounding a fluorophore is known to affect the radiative rate constant k_r. The Einstein *A* and *B* coefficients for absorption and spontaneous emission, respectively, can be used to derive a relationship, between the natural radiative lifetime τ_0 and the absorption and emission spectra of a fluorophore, known as the Strickler Berg formula (Strickler and Berg, 1962)

$$\frac{1}{\tau_0} = k_r = 2.88 \times 10^{-9} n^2 \frac{\int I(\tilde{\nu}) d\tilde{\nu}}{\int I(\tilde{\nu}) \tilde{\nu}^{-3} d\tilde{\nu}} \int \frac{\varepsilon(\tilde{\nu})}{\tilde{\nu}} d\tilde{\nu} \tag{2}$$

in which n is the refractive index, I is the fluorescence emission, ϵ is the extinction coefficient, and $\tilde{\nu}$ is the wavenumber.

The natural radiative lifetime τ_0 and the fluorescence lifetime τ are related through the quantum yield ϕ by

$$\phi = \frac{\tau}{\tau_0} = \frac{k_r}{k_r + k_{nr}} \tag{3}$$

The natural radiative lifetime explicitly depends on the refractive index due to the polarizability of the medium surrounding the fluorophore. Indeed, a number of experimental studies verify the dependence of the natural radiative lifetime τ_0 as well as the fluorescence lifetime τ of dyes on the refractive index (Olmsted III, 1976; Hirayama and Phillips, 1980; Lampert et al., 1983; Hirayama et al., 1990, 1991; Magde et al., 1999), and recently Toptygin et al. (2002) studied the effect of

Submitted April 4, 2002, and accepted for publication July 26, 2002.

Sandrine Lévêque-Fort's present address is Laboratoire de Photophysique Moleculaire, 91405-Orsay cedex, France.

Address reprint requests to Daniel M. Davis, Department of Biological Sciences, Sir Alexander Fleming Building, Imperial College of Science, Technology and Medicine, London SW7 2AZ, UK. Tel.: +44-20-7594-5420; Fax: +44-20-7594-3044; E-mail: d.davis@ic.ac.uk.

© 2002 by the Biophysical Society

0006-3495/02/12/3589/07 $2.00

the refractive index on the radiative rate constant of tryptophan residues. By varying the refractive index with pressure (Hirayama et al., 1991), temperature (Lampert et al., 1983), or by using different solvents (Lampert et al., 1983), the radiative rate constant k_r of anthracene derivatives scales approximately with the square of the refractive index. In addition, the ratio of the natural radiative lifetime in vacuum and in a solvent has been shown to be approximately proportional to the square of the refractive index of the solvent (Hirayama et al., 1990).

Little has been reported on factors that affect the excited state lifetime of the widely used, biologically important GFP. The local pH has been shown not to affect the average fluorescence lifetime of GFP (Heikal et al., 2001). Also, the viscosity of the solvent surrounding the GFP is not a parameter that affects its fluorescence lifetime because no correlation between τ and the viscosity was observed with a variety of solutes added to GFP in buffer (Suhling et al., 2002).

Here, we identify the refractive index as the parameter that does affect the GFP fluorescence decay and demonstrate that the inverse GFP fluorescence lifetime scales approximately with the square of the refractive index. This knowledge is then used to interpret FLIM of GFP in different environments.

MATERIALS AND METHODS

Sample preparation

Polyethylene glycol (average molecular mass 400, AnalaR grade, British Drug Houses, Poole, UK), glycerol (spectrophotometric grade, Sigma-Aldrich, Poole, UK) and NaCl (AnalaR grade, BDH) were mixed with phosphate-buffered saline (PBS) (pH 7.3) in the desired quantities. Mixtures of D(−)fructose (D-levulose, fruit sugar, Sigma-Aldrich) and D(+)glucose (dextrose, corn sugar, Sigma-Aldrich) were used in such a ratio as to cancel out the optical activity. Using a 10-cm path length cuvette placed between two crossed polarizers, this fructose/glucose ratio was found to be 1.50 ± 0.04, independent of the wavelength of the light in the range 430 to 660 nm. Stock solutions of glucose and fructose in aqueous PBS were prepared, mixed in the ratio 1.5:1, and checked for cancellation of the optical activity. The specific rotation was adjusted to 0° ± 1° by titrating stock solutions of glucose or fructose into the mixture. This solution was then diluted with PBS.

For the time-correlated single-photon counting (TCSPC) measurements, 1 μl of 1 mg/ml recombinant enhanced GFP (EGFP, i.e., GFP F64L, S65T, Clontech, Oxford, UK, hereafter referred to as GFP) was added to 0.7 ml of the preprepared mixtures of PBS with different concentrations of glycerol, polyethylene glycol, NaCl, or mixtures of glucose and fructose. This corresponds to a concentration of GFP of 5.3×10^{-8} M. For the multiwell plate imaging, 1 μl of 1 mg/ml GFP was added to 0.1 ml of mixtures of buffer and glycerol, corresponding to a concentration of GFP of 3.7×10^{-7} M. The multiwell plate (Fisher Scientific, Loughborough, UK) is a rectangular array of wells, each having a lateral dimension of 4 mm × 4 mm and a maximal capacity of approximately 100 μl with a transparent plastic base. For the measurements of the absorption and emission spectra to determine the quantum yield, the GFP concentration ranged from 3×10^{-7} M to 8×10^{-7} M.

TCSPC

The fluorescence decays measured with TCSPC (O'Connor and Phillips, 1984) used, as excitation source, a mode-locked tuneable Ti:sapphire laser (Mira 900, Coherent, Watford, UK) pumped by a solid state diode laser (10 W Verdi, Coherent). The optical pulse width was 180 fs. The laser repetition rate of 76 MHz was reduced to 3.8 MHz using a pulse picker (SiO_2 crystal, APE, Berlin, Germany). The excitation wavelength was 470 nm, obtained by frequency doubling the 940-nm laser output after the pulse picker using an angle-tuned barium borate crystal (Ingcrys Laser Systems Ltd, High Wycombe, UK), and the maximal average power at the sample was 20 μW unfocused. The samples were measured in 10-mm path length quartz cuvettes (Hellma Ltd, Southend-on-Sea, UK).

The fluorescence emission was measured at 510 nm using a monochromator with 10-nm bandwidth. The detector was a cooled microchannel plate (Photek Ltd, St. Leonards-on-Sea, UK) operated at −3.4kV, the output pulses of which were passed through a preamplifier into a constant fraction discriminator (Tennelec TC 454 quad CFD, Oxford Instruments, Oakridge, TN). The time to amplitude converter (457 EG&G, Optec, Bracknell, UK) was run in reverse mode, and the stop pulses were furnished by a fast photodiode monitoring the excitation pulses after the pulse picker. By inserting a neutral density filter in the excitation beam path, the stop rate was kept below 1% of the start rate to avoid pulse pile-up (O'Connor and Phillips, 1984). The excitation was vertically polarized, and the emission was collected at the magic angle of 54.7° to avoid rotational depolarization effects on the measured fluorescence (O'Connor and Phillips, 1984). The temperature of the samples was 20°C ± 1°C for all fluorescence decay measurements.

Instrumental response functions, typically 230-ps full-width half maximum, were measured using a Ludox scattering solution (Aldrich, SM30 colloidal silica). The time calibration was typically 29 ps/channel, and 1024 channels were used. Each fluorescence decay was analyzed individually on reconvolution software (IBH, Glasgow, UK).

FLIM

The excitation source is an argon-ion laser pumped mode-locked Ti:Sapphire laser (Tsunami, Spectra-Physics, Hemel Hempstead, UK) operated at a repetition rate of 80 MHz. The output pulses (100 fs) are frequency doubled to 485 nm using a barium borate crystal and coupled into a graded index optical fiber (62.5-μm core diameter, 0.275 N.A., 1-m length, Thorlabs Inc, Newton, NJ). The divergent output at the fiber end (2-mW average power) was reflected from a 45° mirror onto the base of the multiwell plate. The fluorescence was imaged, via the 45° mirror onto a gated high rate image intensifier (Kentech Instruments Ltd, Didcot, UK) after passing through a 500-nm long pass filter to separate the fluorescence emission from the excitation light. The high rate image produced time-gated (full-width half maximum ≈ 400 ps) fluorescence intensity images that were relayed to a 12-bit CCD camera (with 2 × 2 hardware binning (672 × 512 pixels), ORCA-ER, Hamamatsu, Welwyn Garden City, UK) using two front-to-front coupled 50-mm camera lenses (aperture 1:1.8, Nikon, Kingston Upon Thames, UK). Fluorescence lifetime data were obtained by acquiring a series of 15 time-gated fluorescence intensity images at a range of time delays after excitation (Dowling et al., 1999), beginning 400 ps after the fluorescence peak and sampling over 11.5 ns. Each pixel of this set of images was fitted to a single exponential decay profile using a standard nonlinear-least-squares fitting algorithm, and the resulting value for the fluorescence lifetime was displayed on a standard false-color scale. The acquisition, fitting, and display program was written in LabVIEW (National Instruments, Newbury, UK).

Fluorescence quantum yield measurements

The quantum yield of GFP in different solvents, ϕ_x, compared with the quantum yield of GFP in buffer, $\phi_{GFP(buffer)}$, was determined according to

$$\frac{\phi_x}{\phi_{GFP(buffer)}} = \frac{n_x^2}{n_{GFP(buffer)}^2} \frac{F_x}{F_{GFP(buffer)}} \frac{A_{GFP(buffer)}}{A_x} \qquad (4)$$

in which $n_{GFP(buffer)}$, n_x, $F_{GFP(buffer)}$, F_x, $A_{GFP(buffer)}$, and A_x are the refractive index, integrated fluorescence emission spectrum and absorbance of GFP in

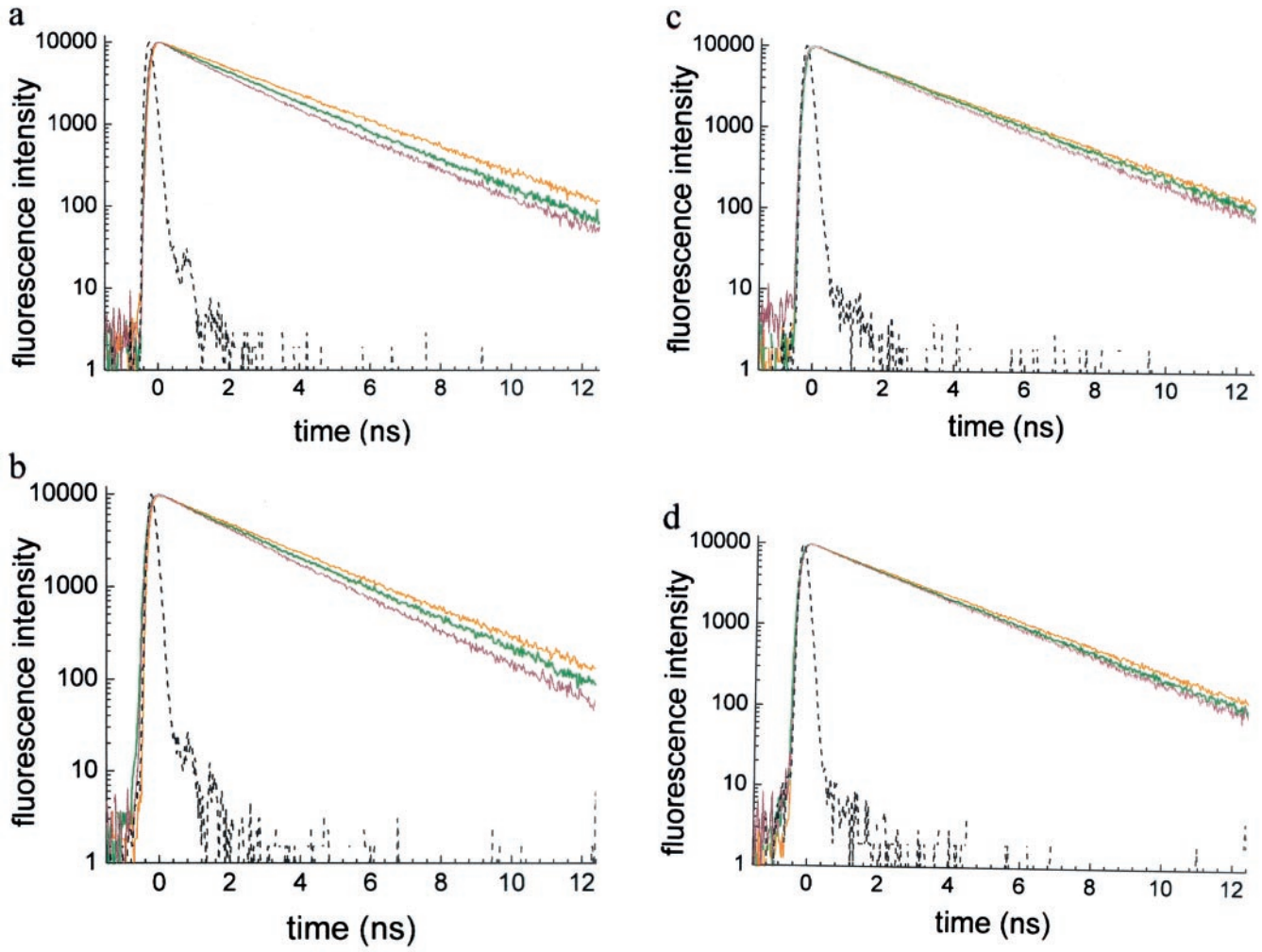

FIGURE 1 Fluorescence decay of GFP is shortened with increasing content of either glycerol, polyethylene glycol, NaCl, or fructose and glucose. The fluorescence decay of GFP (*solid lines*) and the instrumental response to the exciting laser pulse (λ_{ex} = 470 nm, *dashed line*) was measured by TCSPC. (*a*) Semilogarithmic plot of the fluorescence decays of GFP in mixtures of aqueous buffer (PBS, pH 7.3) and glycerol: 0% glycerol (*orange*), 50% glycerol (*green*), and 90% glycerol (*red*). (*b*) Fluorescence decays of GFP in mixtures of aqueous buffer and polyethylene glycol: 0% polyethylene glycol (*orange*), 30% polyethylene glycol (*green*), and 70% polyethylene glycol (*red*). (*c*) Fluorescence decays of GFP in aqueous buffer with added NaCl: 0 g/ml NaCl (*orange*), 0.118 g/ml NaCl (*green*), and 0.248 g/ml NaCl (*red*). (*d*) Fluorescence decays of GFP in aqueous buffer with added fructose and glucose: 0 g/ml fructose and glucose (*orange*), 0.25 g/ml glucose and 0.18 g/ml fructose (*green*), and 0.50 g/ml glucose and 0.36 g/ml fructose (*red*). The fluorescence decays shown are representative of at least four measurements.

buffer, and GFP in other solutions, respectively. Measurements of the fluorescence quantum yield were carried out at two excitation wavelengths, 450 and 470 nm. The absorption and emission spectra were measured on a Shimadzu (Milton Keynes, UK) UV-2501PC spectrophotometer and RF-5301PC spectrofluorophotometer, respectively, using 10-mm path length quartz cuvettes (Hellma Ltd). All measurements were carried out at room temperature.

Refractive index measurements

The refractive index of all solutions was measured using a 60/70 Abbe refractometer (Bellingham and Stanley Ltd, Tunbridge Wells, UK). For 589 nm, the in-built light-emitting diode was used, and the refractive index read off the scale directly. For 510 nm, a halogen lamp with an interference filter was used, and the refractometer calibrated with water for which the wavelength dependence of the refractive index is known (Timmermans, 1950). The readings were then corrected according to the manufacturer's instructions. The calibration and correction were confirmed by measurements of glycerol and found to be in good agreement with tabulated values (Timmermans, 1950). Three readings, each to 4 decimal points, were averaged, and the standard deviation was typically less than to 0.0002. All refractive index measurements were taken at 20°C ± 0.5°C as for the fluorescence decay measurements.

RESULTS AND DISCUSSION

Measurements of GFP fluorescence decays by TCSPC

To study the effect of different environments on the fluorescence decays of GFP, recombinant GFP was added to mixtures

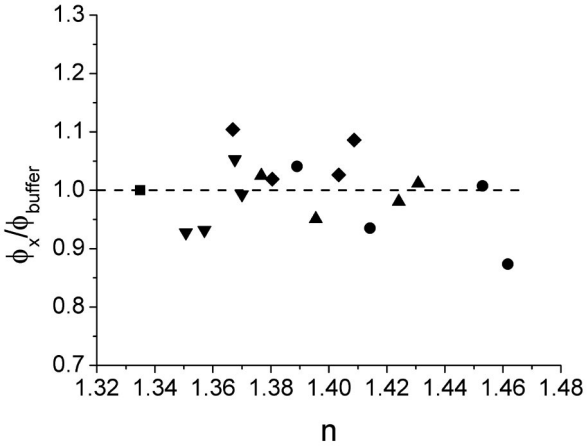

FIGURE 2 Relative quantum yield of GFP in various percentages of solvents, $\phi_x/\phi_{GFP(buffer)}$ (Eq. 4) plotted versus the refractive index n (buffer (■), various concentrations of glycerol (●), polyethylene glycol (▲), NaCl (▼), or fructose and glucose (♦). The error of each data point is estimated by repeated measurements to be 5% to 10%, and the dashed line indicates the average value 1.00 ± 0.06.

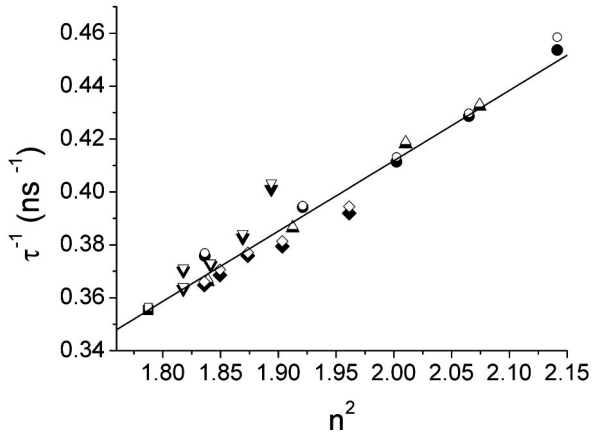

FIGURE 3 Applicability of the Strickler Berg formula (Eq. 1) to the fluorescence decay of GFP. The inverse average fluorescence lifetime $\tau_{av}^{-1} = (a_1\tau_1 + a_2\tau_2)^{-1}$ (a_i being the constant relative amplitudes) of GFP as calculated from a biexponential decay model (*solid symbols*) versus the square of the refractive index of the buffer (■) or various concentrations of glycerol (●), polyethylene glycol (▲), NaCl (▼), or fructose and glucose (♦). τ_{av}^{-1} varies approximately linearly with the square of the refractive index in accordance with the Strickler Berg formula (Eq. 1), irrespective of whether the refractive index is increased by adding glycerol, polyethylene glycol, NaCl, or glucose and fructose. The inverse fluorescence lifetime of GFP from a single exponential fit, τ^{-1}, (*hollow symbols*) is also shown in buffer (□) or various concentrations of glycerol (○), polyethylene glycol (△), NaCl (▽), or fructose and glucose (◇). As the preexponential factors of the biexponential fits are constant, the fit of a monoexponential decay function to the GFP fluorescence decay also reflects the shortening of the fluorescence decay with increasing refractive index. Indeed, the difference between the average fluorescence lifetime τ_{av} and the fluorescence lifetime τ from a single exponential fit is small, and the applicability of the Strickler Berg formula is not affected. Both τ_{av}^{-1} and τ^{-1} increase approximately linearly (—) with the square of the refractive index.

of aqueous buffer with either glycerol, polyethylene glycol, NaCl, or fructose and glucose. Extending our preliminary study (Suhling et al., 2001), it is shown here that the fluorescence lifetime decreases with increasing concentrations of either glycerol, polyethylene glycol, NaCl, or sugar (Fig. 1).

Measurements of the fluorescence decay of GFP using time-correlated single photon counting have previously shown that a monoexponential decay function is not an adequate model to describe the radiative deactivation of the excited state of GFP. This is due to its complex photophysics involving proton transfer kinetics (Cotlet et al., 2001; Heikal et al., 2001), and the use of a two or three exponential decay model, depending on the excitation wavelength, has been proposed (Uskova et al., 2000; Cotlet et al., 2001; Heikal et al., 2001). In agreement with these studies, we also find that a monoexponential decay model does not adequately describe the fluorescence decay of GFP and consistently yields poor values of χ^2 (> 1.35) with systematic deviations in the residuals. A biexponential decay model best fits the GFP fluorescence decay deconvolved from the instrumental response, as judged by the residuals and values of χ^2 (< 1.15). In aqueous solution (PBS, pH 7.3), we measured two lifetimes $\tau_1 = 1.5$ ns and $\tau_2 = 2.9$ ns, with relative amplitudes of 10% and 90%, respectively ($\chi^2 = 1.08$). These two lifetimes τ_1 and τ_2 can be assigned to two different emitting states identified in the absorption spectrum (Cotlet et al., 2001; Heikal et al., 2001).

The relative amplitudes of biexponential fits to the GFP fluorescence decays were found to remain constant upon the addition of glycerol, polyethylene glycol, NaCl, or fructose and glucose and therefore do not vary with refractive index. Thus, a linear combination of the two fluorescence lifetimes (e.g., the average fluorescence lifetime) preserves the same dependence with refractive index as each individual fluorescence lifetime.

However, the Strickler Berg formula (Eq. 2) only applies to the natural radiative lifetime τ_0, and the quantum yield could have an effect on the measured fluorescence lifetime τ (Eq. 3). Therefore, we determined the relative quantum yield of GFP in the solvents used and found no discernible trends (Fig. 2). The maximal variation is no more than 10% over the refractive index range used, and the value for the average relative quantum yield compared with GFP in buffer solution, $\phi_x/\phi_{GFP(buffer)}$ (Eq. 4), is 1.00 ± 0.06. Furthermore, the shape and position of the fluorescence spectra did not change in any of the solutions used.

The inverse average fluorescence lifetime τ_{av}^{-1} scales approximately linearly with the square of the refractive index irrespective of whether the refractive index is altered by the addition of glycerol, polyethylene glycol, NaCl, or glucose and fructose (Fig. 3). τ_{av}^{-1} increases by ~25% over the refractive index range used. As the relative amplitudes of the biexponential fits are constant, the fit of a monoexponential decay function to the GFP fluorescence decay also

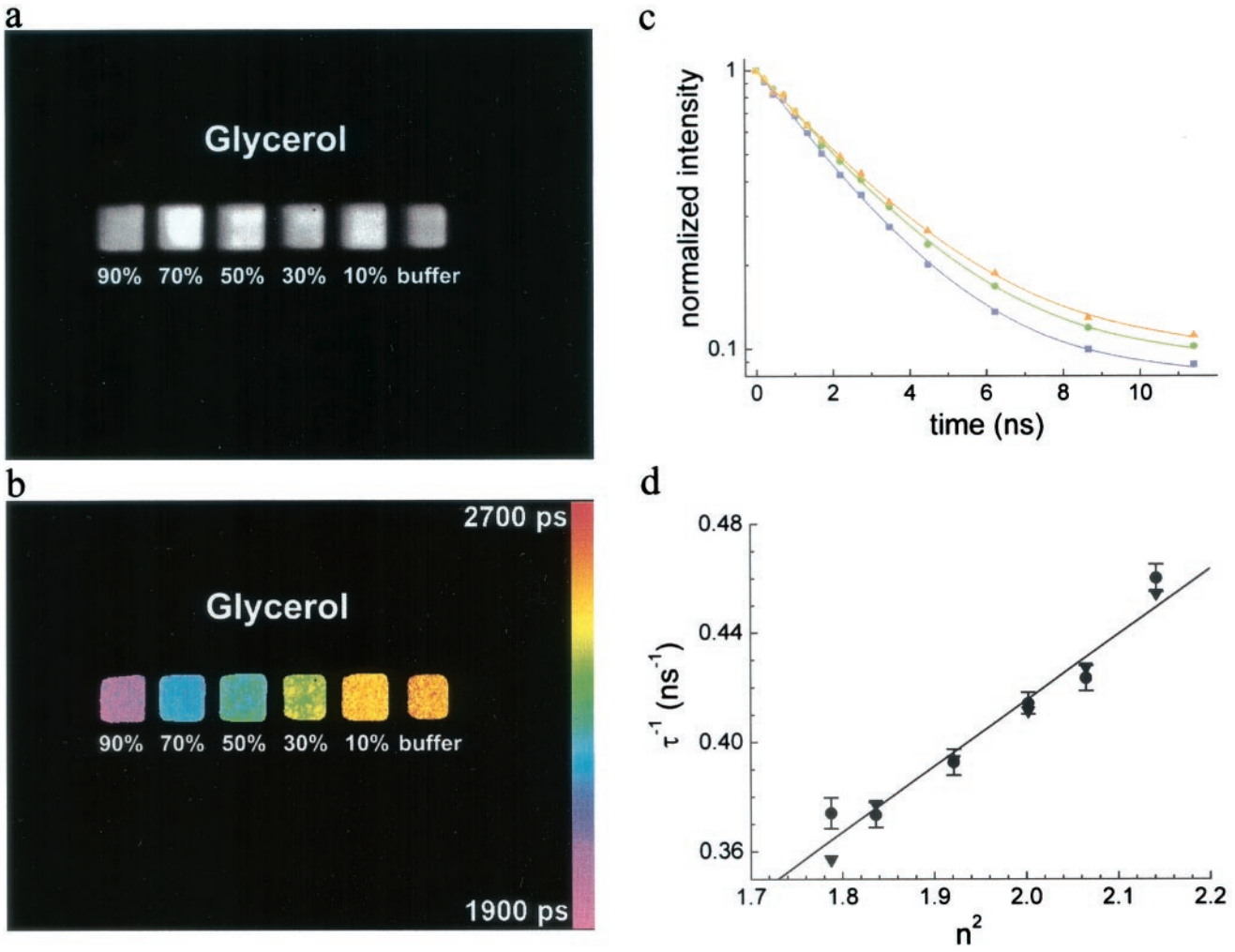

FIGURE 4 GFP fluorescence in mixtures of aqueous buffer and glycerol in a multiwell plate. The figure shows a series of wells filled with GFP in varying percentages of glycerol, as indicated. (*a*) Gated fluorescence intensity image only indicates occupancy of each well. It does not contain information about the GFP environment. (*b*) Corresponding fluorescence lifetime image demonstrates that the technique is sufficiently accurate to detect GFP fluorescence lifetime differences due to the refractive index. Calculating the refractive index in each well according to $n_x = n_{buffer}\sqrt{\tau_{buffer}/\tau_x}$ yields good agreement with direct measurements using a refractometer (Table 1). (*c*) GFP fluorescence decays, in a single pixel, in buffer (▲), 30% glycerol (●), and 70% glycerol (■) are clearly distinguishable. (*d*) Inverse FLIM fluorescence lifetime of GFP (●) and the inverse average fluorescence lifetime of GFP measured by TCSPC (▼) plotted versus the square of the refractive index. For the TCSPC, the standard deviation is less than the size of the data point symbol, and for FLIM the error bars are indicated as standard deviation of the fluorescence lifetime values in each well typically 2%. Figure shown is representative of three independent experiments.

reflects the shortening of the fluorescence decay with increasing refractive index. This is demonstrated in Fig. 3, where the fluorescence lifetime τ from a single exponential fit is shown to be very close to the average fluorescence lifetime τ_{av}. The use of a single exponential decay function in FLIM to fit the fluorescence decay of GFP to report on the refractive index of the GFP environment is therefore tenable.

Recently, Toptygin et al. (2002) studied the radiative rate constant of tryptophan residues as a function of the refractive index of the medium by adding glycerol or sucrose to the buffer. To account for deviations from a strict n^2 dependence of ${\tau_0}^{-1}$, they derived a more complex model than the Strickler Berg equation (Eq. 2) and included shape-dependent depolarization factors and the refractive index of the protein itself. This model describes their experimental results well and yields an effective power dependence of the refractive index in excess of 2. Deviations from the quadratic refractive index dependence have also been discussed by Shibuya (1983a,b). Nonetheless, as Fig. 3 shows, our simple model based on the Strickler Berg equation is adequate to quantitatively describe the dependence of the average fluorescence lifetime of GFP on the refractive index, especially with the accuracy with which the fluorescence lifetime can be imaged using wide-field time-gated FLIM.

TABLE 1 Quantitating the local refractive index by GFP FLIM

	τ (ns)	$n_{calculated}$	$n_{measured}$
PBS	2.67	—	1.337
10% glycerol	2.68	1.34	1.355
30% glycerol	2.55	1.37	1.386
50% glycerol	2.41	1.41	1.415
70% glycerol	2.36	1.43	1.437
90% glycerol	2.17	1.48	1.463

The GFP fluorescence lifetimes, τ, determined by FLIM of a multiwell plate (Fig. 3) can be used to calculate the refractive index of the GFP environment, $n_{calculated}$. The unknown refractive index n_x is calculated from the known refractive index of a buffer, n_{buffer}, and the corresponding fluorescence lifetimes τ_{buffer} and τ_x according to $n_x = n_{buffer}\sqrt{\tau_{buffer}/\tau_x}$, derived from the Strickler Berg formula (Eq. 1). The refractive index determined by this method, $n_{calculated}$, is in good agreement with the refractive index $n_{measured}$ as measured directly with an Abbe refractometer.

FLIM

To demonstrate imaging of the environment of GFP, we imaged recombinant GFP in a series of concentrations of glycerol in a multiwell plate using wide-field time-gated FLIM (Dowling et al., 1999). This technique allows the acquisition of fluorescence decay data in every pixel of an image in parallel, albeit with less temporal resolution and accuracy than TCSPC. Note that with FLIM, we sample the fluorescence intensity at 15 temporal positions, whereas in TCSPC we sample the arrival times of fluorescence photons at 1064 temporal positions.

The fluorescence intensity image merely shows that the wells are occupied (Fig. 4 *a*), and variations in intensity could be due to nonuniform illumination. The intensity image thus does not contain information about the environment of GFP. However, the corresponding FLIM map has contrast due to the GFP fluorescence lifetime, which is a function of the local refractive index of the GFP environment (Fig. 4 *b*). Consistent with TCSPC measurements (Figs. 1 and 3), a gradual decrease of the GFP fluorescence lifetime is evident as the glycerol content, and thus the refractive index is increased. Fluorescence decay curves from individual pixels also clearly show the variation with refractive index (Fig. 4 *c*).

Quantitative analysis to calculate the refractive index n_x from the known refractive index of the buffer n_{buffer}, and the corresponding fluorescence lifetimes τ_{buffer} and τ_x according to $n_x = n_{buffer}\sqrt{\tau_{buffer}/\tau_x}$, is in agreement with the refractive index as measured with an Abbe refractometer (Table 1). The GFP fluorescence lifetimes measured by FLIM and TCSPC also are in good agreement (Fig. 4 *d*). This demonstrates that wide-field time-gated FLIM is sufficiently accurate to distinguish different GFP lifetimes and thus image the refractive index of the local environment of GFP.

The dependence of the fluorescence lifetime on the refractive index has recently been applied to study simple heterogeneous model systems such as reverse micelles (Lavallard et al., 1996; Lamouche et al., 1998, 1999) and liposomes (Toptygin and Brand, 1993; Krishna and Periasamy, 1998) but without imaging. In a biological context, imaging of the refractive index of the environment of specific proteins is novel terrain, but it is known that the cell membrane has a higher refractive index than the cytoplasm, $n_{membrane}1.46 - 1.60$, and $n_{cytoplasm} = 1.35$ (Beuthan et al., 1996; Johnsen and Widder, 1999). This range is larger than the one explored in the present study, and the concomitant fluorescence lifetime changes are thus also expected to be larger (Table 1). Furthermore, it is very likely that different domains within a cell membrane differ in refractive index. However, further studies are needed to interpret changes in the refractive index in cell biology, e.g., using model lipid bilayers and lipid conjugated GFP.

The cutoff distance d at which the radiative rate constant k_r becomes insensitive to the local refractive index is $d \approx 1/(2\,\Delta\nu)$, in which $\Delta\nu$ is the full-width half maximum of the emission spectrum measured in wavenumbers (Toptygin et al., 2002). For GFP, we calculate $d \approx 4\ \mu$m. This can be resolved with our wide-field FLIM microscope with optical sectioning for which a resolution of a few micrometers have been measured experimentally (Webb et al., 2002). As FLIM modules can now be readily attached to commercial microscopes, this new tool for imaging the refractive index may soon be widely used in identifying the environment of specific ligands and receptors tagged with GFP. One application of GFP FLIM would be in live-cell imaging of receptors moving between membrane microdomains of different refractive index as could be the case at immunological synapses (Monks et al., 1998; Grakoui et al., 1999; Davis et al., 1999; Davis, 2002).

The authors would like to thank Leo Carlin for critically reading the manuscript. The work was funded by the United Kingdom's Biotechnology and Biological Sciences Research Council and The Royal Society.

REFERENCES

Bastiaens, P. I. H., and A. Squire. 1999. Fluorescence lifetime imaging microscopy: spatial resolution of biochemical processes in the cell. *Trends Cell Biol.* 9:48–52.

Beuthan, J., O. Minet, J. Helfmann, M. Herrig, and G. Müller. 1996. The spatial variation of the refractive index in biological cells. *Physics Med. Biol.* 41:369–382.

Cotlet, M., J. Hofkens, M. Maus, T. Gensch, M. van der Auweraer, J. Michiels, G. Dirix, M. van Guyse, J. Vanderleyden, A. J. W. G. Visser, and F. C. de Schryver. 2001. Excited state dynamics in the enhanced green fluorescent protein mutant probed by picosecond time-resolved single photon counting spectroscopy. *J. Phys. Chem. B.* 105:4999–5006.

Davis, D. M. 2002. Assembly of the immunological synapse for T cells and NK cells. *Trends Immunol.* 23:356–363.

Davis, D. M., I. Chiu, M. Fassett, G. B. Cohen, O. Mandelboim, and J. L. Strominger. 1999. The human natural killer cell immune synapse. *Proc. Natl. Acad. Sci. U.S.A.* 96:15062–15067.

Dowling, K., M. J. Dayel, S. C. W. Hyde, P. M. W. French, M. J. Lever, J. D. Hares, and A. K. L. Dymoke-Bradshaw. 1999. High resolution

time-domain fluorescence lifetime imaging for biomedical applications. *J. Mod. Optics.* 46:199–209.

Gadella, T. W. J., T. M. Jovin, and R. M. Clegg. 1993. Fluorescence lifetime imaging microscopy (FLIM): spatial-resolution of microstructures on the nanosecond time-scale. *Biophys. Chem.* 48:221–239.

Grakoui, A., S. K. Bromley, C. Sumen, M. M. Davis, A. S. Shaw, P. M. Allen, and M. L. Dustin. 1999. The immunological synapse: a molecular machine controlling T cell activation. *Science.* 285:221–227.

Harpur, A. G., F. S. Wouters, and P. I. H. Bastiaens. 2001. Imaging FRET between spectrally similar GFP molecules in cells. *Nat. Biotechnol.* 19:167–169.

Heikal, A. A., S. T. Hess, and W. W. Webb. 2001. Multiphoton molecular spectroscopy and excited-state dynamics of enhanced green fluorescent protein (EGFP): acid-base specificity. *Chem. Physics.* 274:37–55.

Hirayama, S., Y. Iuchi, F. Tanaka, and K. Shobatake. 1990. Natural radiative lifetime of anthracene derivatives and their dependence on refractive index. *Chem. Physics.* 144:401–406.

Hirayama, S., and D. Phillips. 1980. Correction for refractive index in the comparison of radiative lifetimes in vapour and solution phases. *J. Photochem.* 12:139–145.

Hirayama, S., H. Yasuda, M. Okamoto, and F. Tanaka. 1991. Effect of pressure on the natural radiative lifetimes of anthracene derivatives in solution. *J. Phys. Chem.* 95:2971–2975.

Johnsen, S., and E. A. Widder. 1999. The physical basis of transparency in biological tissue: ultrastructure and the minimization of light scattering. *J. Theor. Biol.* 199:181–198.

Klausner, R. D., A. M. Kleinfeld, R. L. Hoover, and M. J. Karnosvsky. 1980. Lipid domains in membranes. *J. Biol. Chem.* 255:1286–1295.

Krishna, M. M. G., and N. Periasamy. 1998. Fluorescence of organic dyes in lipid membranes: site of solubilization and effects of viscosity and refractive index on lifetimes. *J. Fluoresc.* 8:81–91.

Lakowicz, J. R., H. Szmacinski, K. Nowaczyk, K. W. Berndt, and M. Johnson. 1992. Fluorescence lifetime imaging. *Analyt. Biochem.* 202: 316–330.

Lamouche, G., P. Lavallard, and T. Gacoin. 1998. Spontaneous emission of dye molecules as a function of the surrounding dielectric medium. *J. Luminesc.* 76/77:662–665.

Lamouche, G., P. Lavallard, and T. Gacoin. 1999. Optical properties of dye molecules as a function of the surrounding dielectric medium. *Phys. Rev. A.* 59:4668–4674.

Lampert, R. A., S. R. Meech, J. Metcalfe, D. Phillips, and A. P. Schaap. 1983. The refractive index correction to the radiative rate constant in fluorescence lifetime measurements. *Chem. Physics Lett.* 94:137–140.

Lavallard, P., M. Rosenbauer, and T. Gacoin. 1996. Influence of surrounding dielectrics on the spontaneous emission of sulforhodamine B molecules. *Phys. Rev. A.* 54:5450–5433.

Magde, D., G. E. Rojas, and P. G. Seybold. 1999. Solvent dependence of the fluorescence lifetimes of xanthene dyes. *Photochem. Photobiol.* 70:737–744.

Monks, C. R., B. A. Freiberg, H. Kupfer, N. Sciaky, and A. Kupfer. 1998. Three-dimensional segregation of supramolecular activation in T cell clusters. *Nature.* 395:82–86.

O'Connor, D. V., and D. Phillips. 1984. Time-correlated single photon counting. Academic Press, London.

Olmsted, III J. 1976. Effect of refractive index on molecular radiative lifetimes. *Chem. Physics Lett.* 38:287–292.

Scully, A. D., A. J. MacRobert, S. Botchway, P. O'Neill, R. B. Ostler, and D. Phillips. 1997. Application of fluorescence lifetime imaging microscopy to the investigation of intracellular PDT mechanisms. *Bioimaging.* 5:9–18.

Shibuya, T. 1983a. A dielectric model for the solvent effect on the intensity of light absorption. *J. Phys. Chem.* 78:5175–5182.

Shibuya, T. 1983b. The refractive index correction to the radiative rate constant. *Chem. Physics Lett.* 103:46–48.

Strickler, S. J., and R. A. Berg. 1962. Relationship between absorption intensity and fluorescence lifetime of molecules. *J. Chem. Physics.* 37:814–820.

Suhling, K., D. M. Davis, Z. Petrášek, J. Siegel, and D. Phillips. 2001. The influence of the refractive index on EGFP fluorescence lifetimes in mixtures of water and glycerol. *Proc. S.P.I.E.* 4259:92–101.

Suhling, K., D. M. Davis, and D. Phillips. 2002. The influence of solvent viscosity on the fluorescence decay and time-resolved anisotropy of green fluorescent protein. *J. Fluoresc.* 12:91–95.

Sullivan, K. F., and S. A. Kay, editors. 1999. Green Fluorescent Proteins Methods in Cell Biology. Academic Press, San Diego, CA.

Timmermans, J. 1950. Physico-Chemical Constants of Pure Organic Compounds. Elsevier, New York.

Toptygin, D., and L. Brand. 1993. Fluorescence decay of DPH in lipid membranes: influence of the external refractive index. *Biophys. Chem.* 48:205–220.

Toptygin, D., R. S. Savtchenko, N. D. Meadow, S. Roseman, and L. Brand. 2002. Effect of the solvent refractive index on the excited-state lifetime of a single tryptophan residue in a protein. *J. Phys. Chem. B.* 106: 3724–3734.

Tsien, R. Y. 1998. The green fluorescent protein. *Annu. Rev. Biochem.* 67:509–544.

Uskova, M. A., J. Borst, M. A. Hink, A. van Hoek, A. Schots, N. L. Klyachko, and A. J. W. G. Visser. 2000. Fluorescence dynamics of green fluorescent protein in AOT reversed micelles. *Biophys. Chem.* 87: 73–84.

Verveer, P. J., F. S. Wouters, A. R. Reynolds, and P. I. H. Bastiaens. 2000. Quantitative imaging of lateral ErbB1 receptor signal propagation in the plasma membrane. *Science.* 290:1567–1570.

Wang, X. F., A. Periasamy, B. Herman, and D. M. Coleman. 1992. Fluorescence lifetime imaging microscopy (FLIM): Instrumentation and applications. *Crit. Rev. Analyt. Chem.* 23:369–395.

Webb, S. E. D., Y. Gu, S. Lévêque-Fort, J. Siegel, M. J. Cole, K. Dowling, R. Jones, P. M. W. French, M. A. A. Neil, and R. Juškaitis. 2002. A wide-field time-domain fluorescence lifetime imaging microscope with optical sectioning. *Rev. Sci. Instrum.* 73:1898–1907.

Zimmer, M. 2002. Green fluorescent protein (GFP): applications, structure, and related photophysical behavior. *Chem. Rev.* 102:759–782.